Available online at www.sciencedirect.com
ScienceDirect
Applied Surface Science 253 (2007) 5017–5028
applied surface science
www.elsevier.com/locate/apsusc

The absorptance of steels to Nd:YLF and Nd:YAG laser light at room temperature

D. Bergström [a,*], J. Powell [b], A.F.H. Kaplan [c]

[a] Department of Engineering, Physics and Mathematics, Mid Sweden University, Östersund, Sweden
[b] Laser Expertise Ltd., Nottingham, UK
[c] Luleå University of Technology, Luleå, Sweden

Received 18 August 2006; received in revised form 7 November 2006; accepted 7 November 2006
Available online 14 December 2006

Abstract

The measurement of absorptance is important for the analysis and modelling of laser–material interactions. Unfortunately, most of the absorptance data presently available considers only polished pure metals rather than the commercially available (unpolished, oxidised) alloys, which are actually being processed in manufacturing. This paper presents the results of absorptance measurements carried out at room temperature on as-received engineering grade steels including hot and cold rolled mild steel and stainless steels of various types. The measurements were made using an integrating sphere with an Nd:YLF laser at two wavelengths (1053 and 527 nm, which means that the results are also valid for Nd:YAG radiation at 1064 and 532 nm). The absorptance results obtained differ considerably from existing data for polished, pure metals and should help improve the accuracy of laser–material interaction models. Some clear trends were identified; for all materials studied, the absorptance was considerably higher than the previously published values for the relevant pure metals with polished surfaces. For all 15 samples the absorptance was higher for the green than for the infrared wavelength. No clear trend correlating the absorptance with the roughness was found for mild steel in the roughness range Sa 0.4–5.6 μm. A correlation between absorptance and roughness was noted for stainless steel for Sa values above 1.5 μm.

PACS : 42.62.-b; 42.82.-m; 78.66.Bz; 78.68.+m

Keywords: Laser material processing; Absorptance; Steels; Integrating sphere

1. Introduction

In laser material processing of metals, an understanding of the fundamental absorption mechanisms plays a vital role in determining the optimum processing parameters and conditions. The absorptance[1], which is the fraction of the incident laser light which is absorbed, depends on a number of different parameters, the most important of which are listed in Table 1 [1–4].

When modelling laser processing applications, such as cutting, welding, drilling, cladding, hardening, etc., it is important to model the absorption correctly. In very sophisticated models, it may be necessary to have an analytical function for the different absorption mechanisms. In other, simpler, cases it may be sufficient to have an accurate average absorptance value to plug in. In any case, published data for the absorptance and reflectance of metals are usually presented only for perfectly pure, clean and flat surfaces, which are free from oxide layers (measurements are commonly done in vacuum). This is quite different from the normal situation found in a real life material processing applications. Most metal surfaces are rough to some extent and oxide layers are more of a rule than an exception. Also, the concentration on pure metals has meant that there is very little information available for the absorptance of alloys (stainless steel, brass, etc.), polished or otherwise. In real processing environments alloys are far more commonly used than pure metals. It is therefore generally inappropriate to use the published values of absorptance for pure polished surfaces in mathematical models of laser processing.

* Corresponding author. Tel.: +46 63 165911; fax: +46 63 165500.
E-mail address: david.bergstrom@miun.se (D. Bergström).

[1] Also known as absorptivity. NIST recommends using the word absorptivity for perfectly flat and pure surfaces and absorptance for rough and contaminated surfaces (i.e. all real surfaces).

0169-4332/$ – see front matter © 2006 Elsevier B.V. All rights reserved.
doi:10.1016/j.apsusc.2006.11.018

Table 1
Laser and metal properties of importance to absorption [1–4]

Laser properties	Metal properties
Wavelength	Chemical composition
Polarization	Temperature
Angle of incidence	Roughness/topography
Intensity, non-linear effects	Oxide layers
	Contamination (dust, dirt, surface, bulk defects, etc.)

Fig. 1 demonstrates some of the complexities of photon absorption by an engineering grade metal surface. Such a surface has a characteristic roughness and is always covered by an oxide layer. The surface roughness can result in multiple reflections, which involve multiple absorption events (Fig. 1b). Surface roughness can also involve the incoming radiation in absorption events at high angles of incidence, close to the Brewster angle. This can result in very high local absorptance levels. The oxide layer may be absorbing in its own right or may be responsible for multiple reflections or wave guiding (Fig. 1c). In addition to these effects the surface may be contaminated with material which has a higher absorptance than the underlying metal.

All of the above phenomena increase the absorptance of the surface in question and the use of alloying elements will also tend to complicate the situation. For this reason, the best way to establish the absorptance of an engineering metal surface is by direct measurement.

It is, of course, extremely difficult to measure the absorptance of the molten, turbulent surfaces typical of laser welding or cutting. However, it is possible to accurately measure the absorptance of the solid material at room temperature and the values obtained can provide an insight into how the materials behave at elevated temperatures. This can be argued from the fact that, for wavelengths around 1 μm, the temperature dependence of absorptance is small. It is well established that metals usually have a so called X-point, a wavelength point or band where the temperature coefficient of absorptance changes sign [5]. The reason for this kind of behaviour lies in the different temperature coefficients for intraband (free electron) and interband (bound electron) absorption, the two intrinsic absorption mechanisms prevalent in metals. Intraband absorption increases with temperature, simply because the free electrons gain kinetic energy while the phonon population grows, which increases the electron–phonon collision frequency (i.e. the energy conversion efficiency between the light, the free electrons and the lattice). Interband absorption, on the other hand, is much more complicated and depends on the particular band structure of the metal. The general principle is that as the temperature is elevated, the electron Fermi energy distribution function is smoothed out and the absorption bands are broadened. The competition between these two effects leads to the X-point, which for most metals lies near 1 μm [6].

In any case, the absorptance of the solid material as opposed to the molten state is, in itself, very important for two reasons:

(1) During the initiation of any weld or cut the laser is interacting with the solid surface.
(2) During welding or cutting the leading edge of the laser beam in many cases interacts with the solid surface of the material.

This paper presents the results of an experimental survey of the room temperature absorptance of a wide range of commercially available steels in the as-received state.

A comprehensive literature survey with 46 references on experimental absorption measurement methods is given in Ref. [7] by the present authors. In addition, the present authors have provided a comprehensive literature survey on theory and

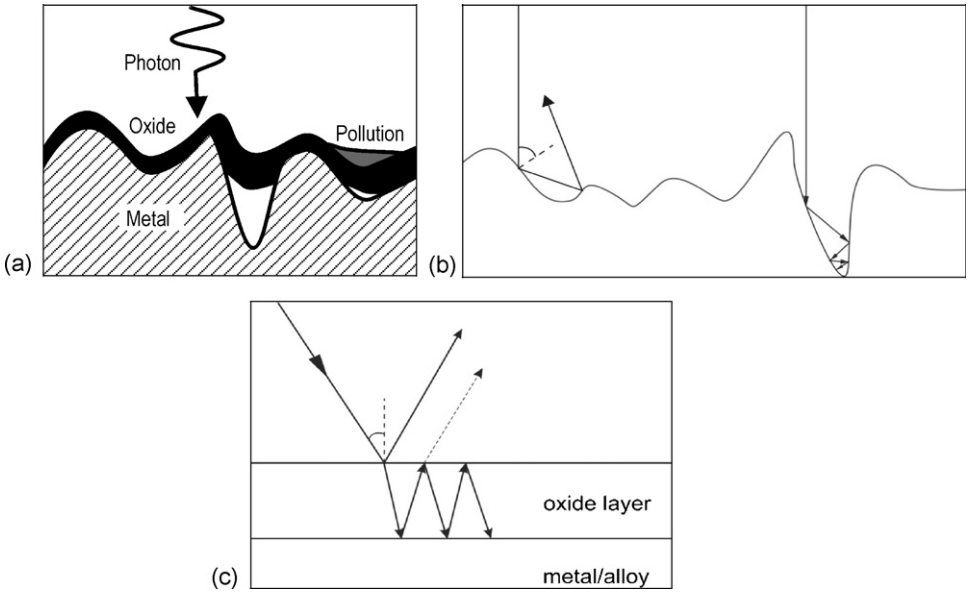

Fig. 1. Some of the mechanisms which increase the absorptivity of real engineering surfaces: (a) typical cross section of an engineering surface; (b) high (Brewster) angle absorptance and multiple reflections due to surface roughness and (c) multiple reflections within an oxide layer.

modelling of the absorption mechanism in metals in Ref. [1], with reference to 47 publications. General treatments of laser absorption mechanisms can be found in Ref. [1–4].

There are a number of different experimental methods available for measuring laser absorptance in opaque solids. Some of the more commonly used are; laser calorimetry, gonioreflectometry, integrating sphere or integrating mirror reflectometry and emittance spectroscopy [7–9].

In this paper, reflectometry using an integrating sphere was selected, mainly because integrating spheres are commercially available, relatively inexpensive and easy to use while at the same time being very accurate and versatile. By measuring the reflectance R of a sample, we get immediate information regarding the absorptance A, since $A = 1 - R$ for opaque solids.

2. Experimental setup

2.1. Instrumentation

The reflectance measurements were carried out in the laser laboratory at the Mid Sweden University, in Östersund. The laser used as the radiation source was a 1 W cw Nd:YLF laser with a fundamental wavelength 1053 nm, equipped with a Second Harmonic Generation (SHG) crystal to also allow production of green light at 527 nm.

The reflectance of the various metals was measured by using an integrating sphere in a double beam setup, as shown in Fig. 2. The 150 mm diameter 6-port integrating sphere has a barium sulphate based coating called Spectraflect, which has high reflective Lambertian properties for wavelengths between 300 and 2400 nm.

The Nd:YLF laser beam was directed onto a rotatable mirror (M2 in Fig. 2) that was flipped between two positions to produce sample and reference beams. The flipping frequency was set to approximately 1 Hz, to ensure mirror stability. Mirrors 3 and 4 (M3 and M4 in Fig. 2) then directed the beams onto the sample and reference, respectively, at an angle of incidence of 8°. As reference a port plug of Spectraflect was used. After spatial integration by the sphere, the reflected light was then detected by a reverse biased 5.7 mm^2 Si photodiode, with a spectral response between 190 and 1100 nm. The voltage signal of the photodiode was finally digitized in an A/D-converter and sampled by a PC.

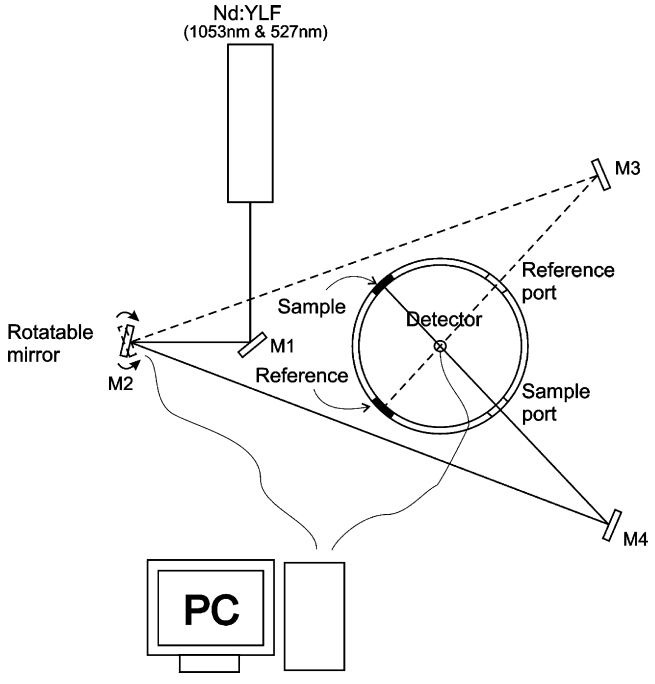

Fig. 2. The experimental setup for measuring reflectance.

2.2. Error correction methods

Several correction methods were applied to the reflectance measurements to improve accuracy and minimize errors. Clarke and Compton [10] have identified the following main sources of errors in integrating sphere reflectometers:

(a) Light losses through ports in the sphere wall,
(b) Unequal illumination of the sample and standard and changes in throughput when a single beam method is used,
(c) Directional dependence of light scattering from the sample and standard surfaces,
(d) Errors due to diffraction effects in apertures,
(e) Errors due to imperfect diffusion of reflected light from the sphere walls (non-lambertian characteristics) and
(f) Baffling.

To minimize these errors the following procedures and correction methods were applied to the measurements:

(a) Light losses:
With the aim of reducing light losses, all ports not in use were closed with port plugs.
(b) Unequal illumination of sample and standard:
The double beam configuration used in these experiments avoids the substitution error, which is often a feature of single beam measurements (and can be as large as 4–5% according to the manufacturers [11]). The double beam configuration also has the advantage of reducing the influence of possible laser power fluctuations.
(c) Directional dependence of light scattering:
Light behaves slightly different inside the sphere when reflected from a rough surface as compared to a relatively flat one. Light incident on a flat surface is subjected to mirror-like, specular reflection in contrast to rough surfaces where the reflected light is scattered diffusively into many different directions. This produces differences in the number of reflections needed inside the sphere before the light is homogenously scattered, which will lead to detector throughput changes. This error can be corrected for by using a combination of diffuse (rough) and specular (flat) reflectance standards.

By knowing the sample diffusivity, D_s, which is the fraction of reflected light which is scattered diffusively (specular part excluded), the reflectance of the sample, R_s,

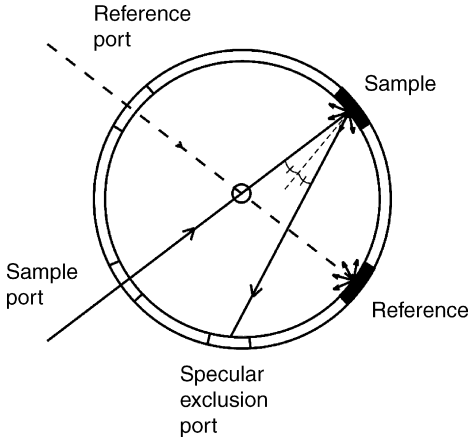

Fig. 3. Diffusivity can be measured by excluding the specular fraction of the reflected light, through an empty port or by fitting a light trap.

can then be obtained by

$$R_s = S_s\left[\left(1 - D_s\right)\frac{R_{s,r}}{S_{s,r}} + D_s\frac{R_{d,r}}{S_{d,r}}\right], \quad (1)$$

where S_s is the signal measured with the sample, $R_{s,r}$ the reflectance of the specular standard (mirror), $S_{s,r}$ the signal measured with the specular standard, $R_{d,r}$ the reflectance of the diffuse standard and $S_{d,r}$ is the signal measured with the diffuse standard [12].

The diffusivity can be measured by opening the specular exclusion port (or attaching a light trap) and comparing the signal from the sample to a signal from the diffuse standard, see Fig. 3. The diffusivity is then given by

$$D_s = 1 - \frac{S_{s,spex}/S_s}{S_{d,spex}/S_{d,r}}, \quad (2)$$

where $S_{s,spex}$ is the signal measured with sample and with specular exclusion port opened and $S_{d,spex}$ is the signal measured with the diffuse standard and specular exlusion port opened. Using this method, a diffusivity of 100% was assigned to the diffuse standards and 0% to the specular mirror standard. This error was empirically seen to be almost negligible for $\lambda = 527$ nm, but could amount to more than 1% in absolute reflectance for $\lambda = 1053$ nm.

Table 3
Surface conditions of the 15 samples studied

No.		Surface	Sa [μm]	Sq [μm]
	Mild steels			
MS1	CR4	Cold rolled	0.92	1.16
MS2	CR4	Cold rolled	1.45	1.68
MS3	43A	Hot rolled	1.73	2.17
MS4	43A	Hot rolled	0.46	0.58
MS5	43A	Hot rolled	1.24	1.51
MS6	43A	HR, pickled, oiled	2.68	3.23
MS7	43A	HR, corroded	5.58	6.47
	Stainless steels			
SS1	304SS	Cold rolled	0.29	0.34
SS2	316SS	Cold rolled	0.15	0.19
SS3	304SS	Hot rolled	3.26	4.17
SS4	316SS	Hot rolled	2.25	3.57
SS5	3Cr12	Hot rolled	2.47	3.48
SS6	304SS	Bright annealed	0.09	0.12
SS7	430SS	Bright annealed	0.05	0.08
SS8	316SS	Dull polished (brushed)	1.38	1.83

(d) Diffraction effects in apertures:

To get a suitable laser spot size on the sample, a lens was put in front of the sample beam entrance port. Due to diffraction, this produces a characteristic halo around the sample and sample port, which causes a slight error to the measurements. Empirically this was shown to be around 0.2% in absolute reflectance. This error was easily corrected for by measuring the signal with the sample port empty and subtracting this from the signal with the sample in place.

Errors (e) and (f) are due to the specific sphere designs and are not easily corrected for.

Another error was identified in the case of structured samples with contoured surfaces (termed 'lay' in the literature on surface properties). According to Roos et al. [13] this error can be substantial if care is not taken in positioning the samples correctly in the sample ports. A contoured surface produces a reflected band of light (termed specular-diffuse radiation by Roos et al. [13]), which will produce errors if the band crosses the detector (giving too high a reflectance value) or passes through any open beam ports (giving too low a reflectance value). No other corrections than correct positioning was applied in this case.

Table 2
List of the steels examined in this survey and their chemical composition

No.		Fe[a] (%)	C[a] (%)	Cr[a] (%)	Ni[a] (%)	Mn[a] (%)
	Mild steels					
MS1–MS2	CR4	99.0	0.1	0.0	0.0	0.6
MS3–MS7	43A, DIN 17100, St44-2	98.0	0.2	0.0	0.0	1.5
	Stainless steels					
SS1, SS3, SS6	AISI 304SS, DIN 1.4301	70.4	0.0	18.0	9.5	2.0
SS2, SS4, SS8	AISI316SS, DIN 1.4401	68.4	0.0	17.0	12.5	2.0
SS5	AISI3Cr12, DIN 1.4003	88.0	0.0	11.5	0.5	0.0
SS7	AISI430SS, DIN 1.4016	81.4	0.0	17.0	0.5	1.0

[a] wt.%.

The measurements were performed in a dark room to minimize the influence of external light sources, such as lamps. Corrections were also made to the current flowing through the photodiode in absence of light. These dark current measurements were performed before each measurement, which were then subtracted from the measured signals.

Using the correction methods outlined above, the reflectance values of all the diffuse and specular standards were seen to be reproducible to at least within 0.3% in absolute reflectance. The same reliability can approximately be attributed to the following results for the samples investigated.

2.3. Samples and measurements

Table 2 lists the different samples of steels (ferrous samples) examined in the survey in terms of their standards denominations and their chemical composition. Note that a similar study on aluminium alloys, copper alloys and zinc-coatings was also carried out and is under preparation as a separate publication.

The corresponding technical surfaces for the 15 samples studied are described in Table 3. The roughness values given in this table are supported by SEM and optical microscopy together with profilometry imaging in the results section of this work.

The standard engineering phrases, which describe the surface condition of the steels (hot rolled (HR), pickled, oiled, etc.) need some explanation here;

Mild steel—cold rolled; in this case the as-received material has a surface, which has a microscopic surface texture as a result of the rolling process. Cold rolled mild steel has a clean surface, which is covered in a very thin layer of oxide, which is transparent to the naked eye. (The material is also usually

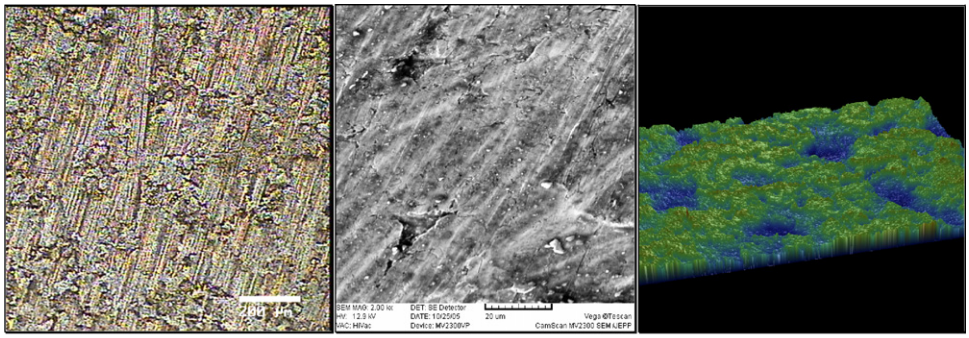

λ=1053nm		λ=532nm	
A	σ	A	σ
62.0%	2.2%	71.8%	1.5%

Sa[μm]	0.92	Sq[μm]	1.16

(a)

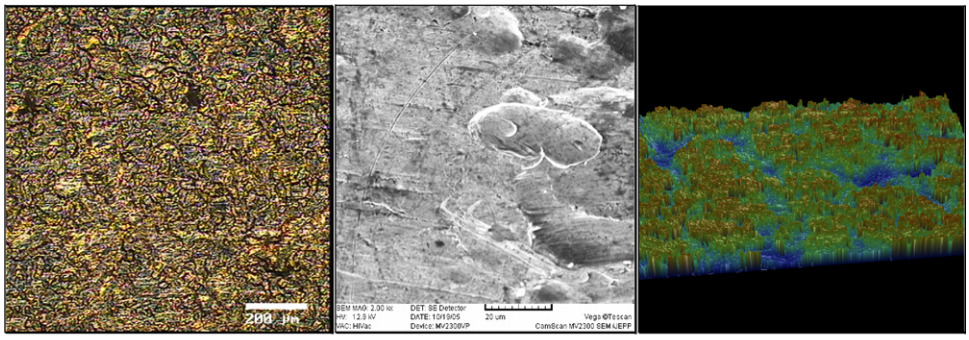

λ=1053nm		λ=532nm	
A	σ	A	σ
48.1%	1.4%	64.4%	0.5%

Sa[μm]	1.45	Sq[μm]	1.68

(b)

Fig. 4. Cold rolled mild steel: (a) MS1: CR4 and (b) MS2: CR4.

coated in a thin layer of oil, which was removed prior to absorptance testing.) The material is approximately 99% pure iron.

Mild steel—hot rolled; hot rolled mild steel is covered in a material called 'Mill Scale' which is an oxide layer several tens of microns deep. The laser therefore interacts primarily with

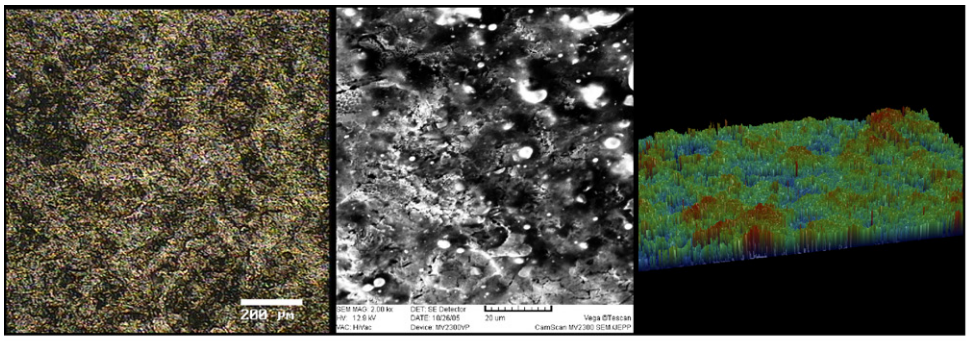

λ=1053nm		λ=532nm	
A	σ	A	σ
84.3%	0.6%	91.2%	0.0%

Sa[μm]	1.73	Sq[μm]	2.17

(a)

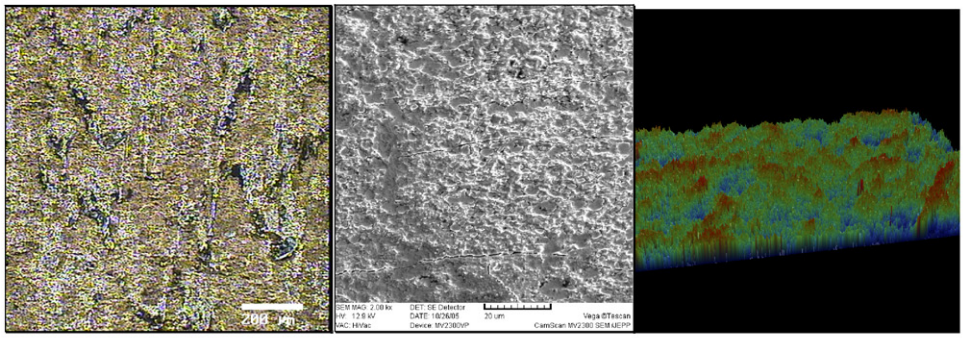

λ=1053nm		λ=532nm	
A	σ	A	σ
81.4%	0.4%	82.3%	0.1%

Sa[μm]	0.46	Sq[μm]	0.58

(b)

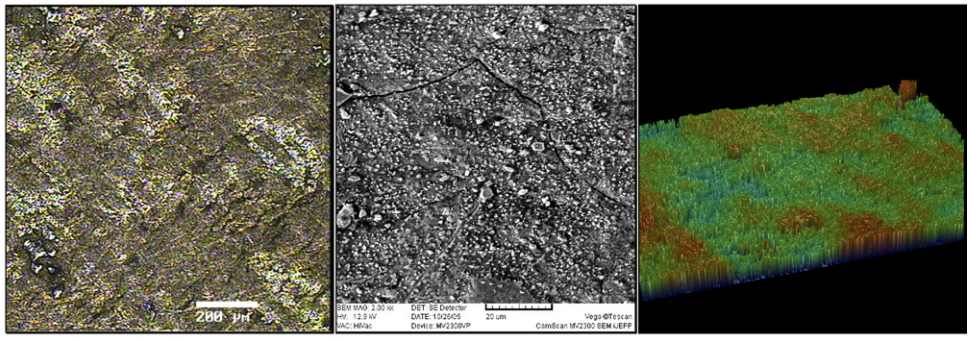

λ=1053nm		λ=532nm	
A	σ	A	σ
86.8%	0.2%	88.8%	0.0%

Sa[μm]	1.24	Sq[μm]	1.51

(c)

Fig. 5. Hot rolled mild steel: (a) MS3: 43A; (b) MS4: 43A and (c) MS5: 43A.

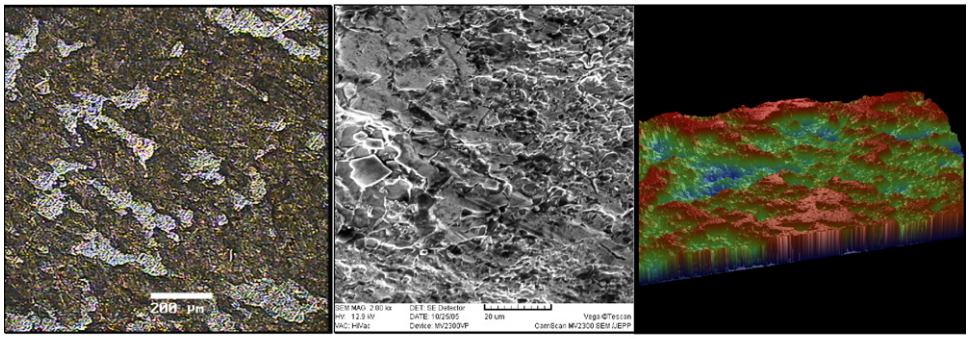

λ=1053nm		λ=532nm	
A	σ	A	σ
67.8%	0.7%	78.1%	0.5%

Sa[μm]	2.68	Sq[μm]	3.23

Fig. 6. MS6: mild steel 43 A, hot rolled, pickled and oiled.

this surface mixture of iron oxides rather than the underlying 98% iron alloy.

Mild steel—hot rolled, pickled and oiled; mild steel in this condition has been hot rolled to the required thickness and subsequently 'Pickled' in acid to remove the 'mill scale' oxide surface. After pickling, the sheets of steel are coated in oil as a protection against corrosion (This oil was, of course, removed prior to our reflectance measurements). The surface texture of this material is rougher than that of cold rolled mild steel. The surface can also have residual pockets of oxide in some of the deeper surface pits (see Fig. 1).

Mild steel—hot rolled, corroded; cold rolled and hot rolled pickled and oiled mild steel is coated in oil and therefore resistant to corrosion during storage. Hot rolled material is corrosion resistant as a result of its surface layer of oxides. However, if hot rolled mild steel is stored outside for any length of time, it can accumulate a patchy layer of brown corrosion products because water can penetrate the oxide layer. As part of this survey of as-received engineering grade steels we included samples of partially corroded hot rolled steel.

Stainless steel—cold rolled; this material has a clean, microscopically textured surface.

Stainless steel—hot rolled; unlike its mild steel counterpart, hot rolled stainless steel is not coated with oxides as a result of the rolling process. Hot rolled stainless does, however, have a rougher surface texture than the cold rolled material.

Stainless steel—bright annealed; as the name implies, this grade of stainless steel has been rolled to produce a bright, almost mirror quality surface.

Stainless steel—dull polished (Brushed). This grade of stainless steel has been surface ground in one direction to give the 'brushed' finish commonly used in display work, hotel bars, etc.

The samples were laser or mechanically cut from sheets into 30 mm squares with thicknesses varying between 2 and 6 mm.

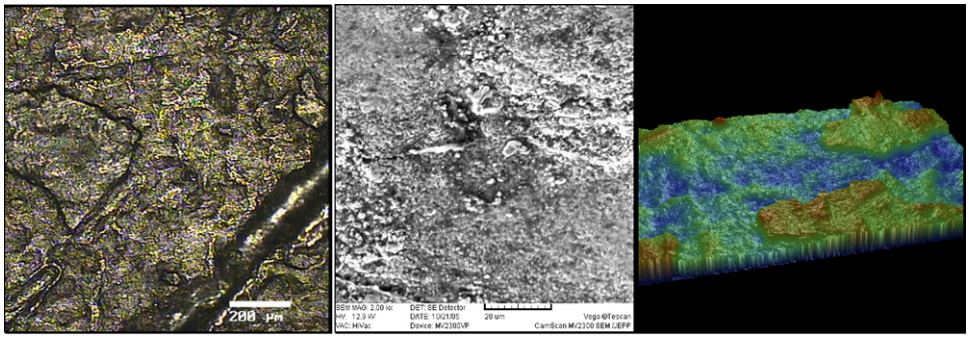

λ=1053nm		λ=532nm	
A	σ	A	σ
87.6%	1.3%	90.5%	1.5%

Sa[μm]	5.58	Sq[μm]	6.47

Fig. 7. MS7: mild steel 43A, hot rolled and corroded.

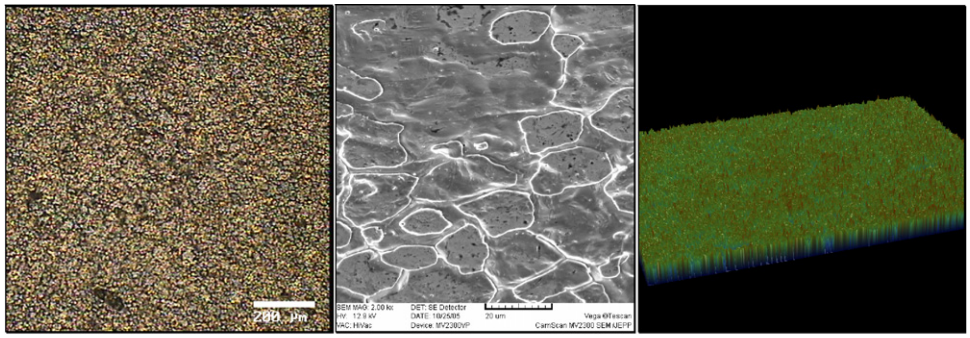

λ=1053nm		λ=532nm	
A	σ	A	σ
37.4%	0.3%	44.6%	0.2%

(a)

Sa[μm]	0.29	Sq[μm]	0.34

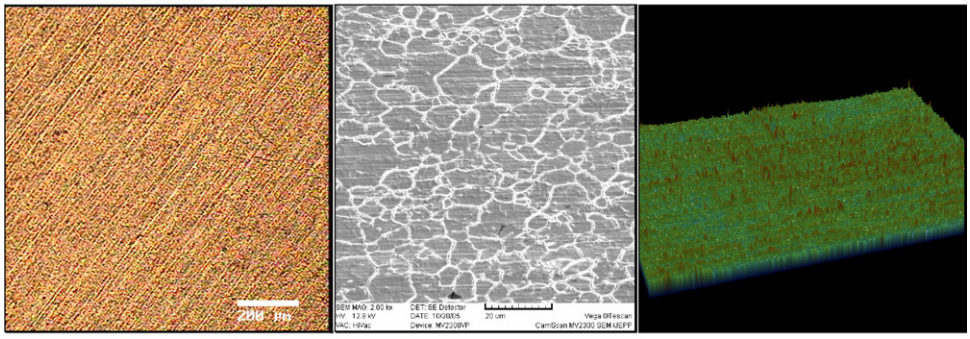

λ=1053nm		λ=527nm	
A	σ	A	σ
37.2%	0.3%	43.8%	0.3%

(b)

Sa[μm]	0.15	Sq[μm]	0.19

Fig. 8. Cold rolled stainless steel: (a) SS1: 304SS and (b) SS2: 316SS.

For each sample, measurements were taken at five separate locations, which were then averaged and a standard deviation was calculated. Each measurement for every location is in turn an average of over 300 data points.

All integrating sphere measurements are done relative to a standard of known reflectance. In these experiments, a combination of diffuse and specular reflectance standards were utilized. The diffuse standards had reflectances between 2 and 99%. The specular standard consisted of an Al-coated mirror, which was calibrated at the Ångström Laboratory in Uppsala, Sweden. It had a reflectance of 97.7% at 1053 nm and 98.9% at 527 nm.

The reliability of the absorptance measurement method was regarded as satisfactory. The variance σ of the measured A values was low. In 17 of 30 cases (15 material samples, 2 wavelengths) the variance of the five measurements was less than 1.5%, only in 1 case (SS3, IR) it was higher than 10%.

2.4. Equipment for surface characterization

For characterizing the surfaces of the different samples investigated in this study, a Nikon Eclipse L200 optical microscope, a CamScan MV2300T Scanning Electron Microscope (SEM) and a Wyko NT1100 optical profiler were used. The optical profiler, used for measuring the roughness of the sample surfaces, had a horizontal resolution of 1.6 μm and a vertical resolution in the sub-nanometer range.

3. Results

Figs. 4–7 for mild steel and Figs. 8–10 for stainless steel present the optical microscopy (OM), Scanning Electron Microscope, profilometry and absorptance results obtained in this survey. In each figure, the magnification used is 100 times for the optical microscopy pictures, 2000 times for the SEM photos and 5 times for the 3-D optical profilometry scans.

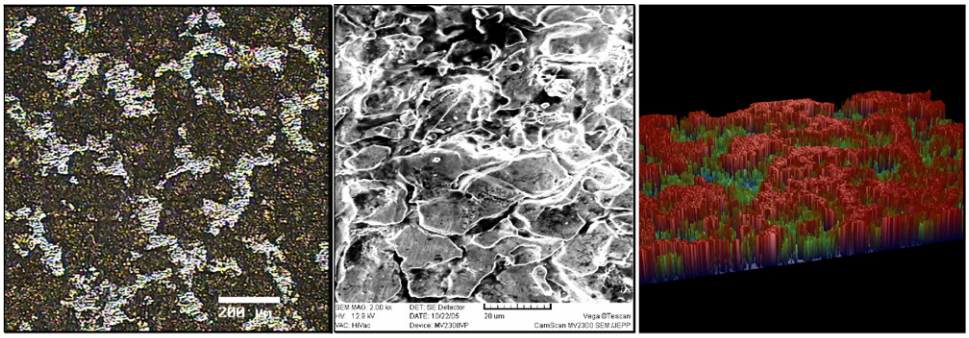

λ=1053nm		λ=527nm	
A	σ	A	σ
57.5%	3.2%	65.2%	2.7%

Sa[μm]	3.26	Sq[μm]	4.17

(a)

λ=1053nm		λ=532nm	
A	σ	A	σ
54.6%	9.4%	64.1%	6.5%

Sa[μm]	2.25	Sq[μm]	3.57

(b)

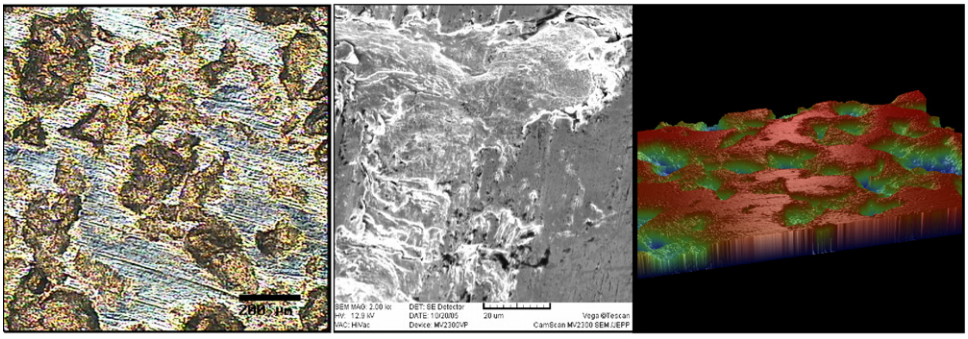

λ=1053nm		λ=527nm	
A	σ	A	σ
44.2%	1.8%	54.8%	3.8%

Sa[μm]	2.47	Sq[μm]	3.48

(c)

Fig. 9. Hot rolled stainless steel: (a) SS3: 304SS; (b) SS4: 316SS and (c) SS5: 3Cr12.

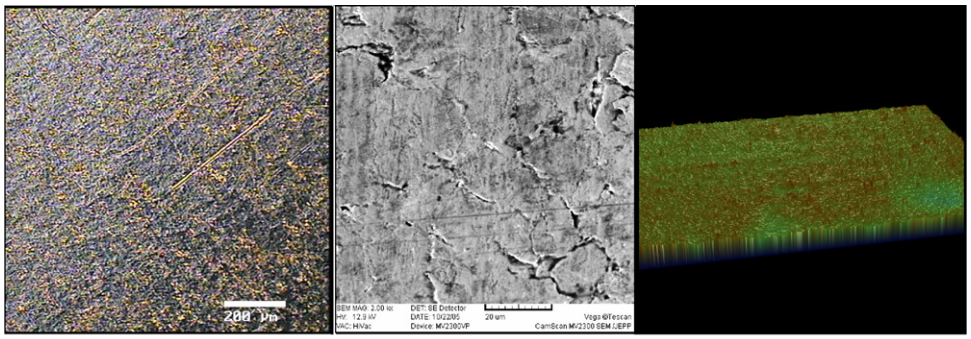

λ=1053nm		λ=527nm	
A	σ	A	σ
32.4%	0.2%	42.9%	0.8%

Sa[μm]	0.09	Sq[μm]	0.12

(a)

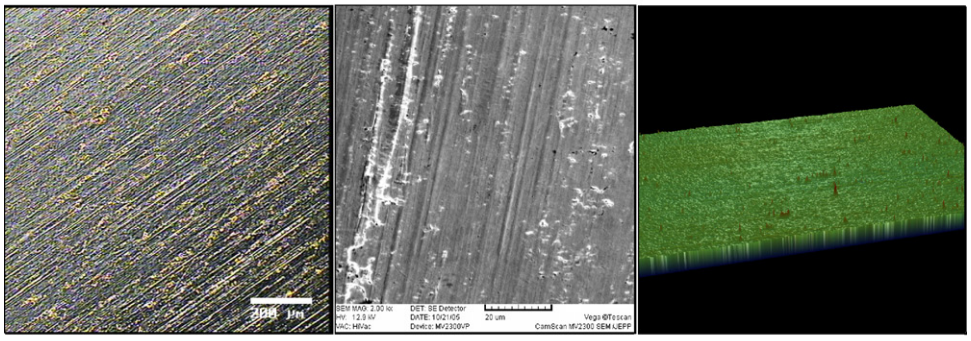

λ=1053nm		λ=527nm	
A	σ	A	σ
37.0%	0.3%	48.9%	0.3%

Sa[μm]	0.05	Sq[μm]	0.08

(b)

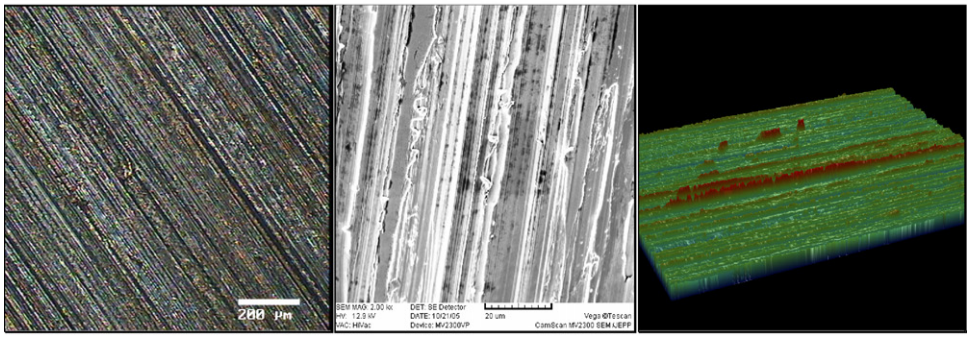

λ=1053nm		λ=527nm	
A	σ	A	σ
37.3%	2.3%	45.4%	2.5%

Sa[μm]	1.38	Sq[μm]	1.83

(c)

Fig. 10. Specially prepared stainless steel surfaces: (a) SS6: 304SS, bright annealed; (b) SS7: 430SS, bright annealed and (c) SS8: 318SS, dull polished (brushed).

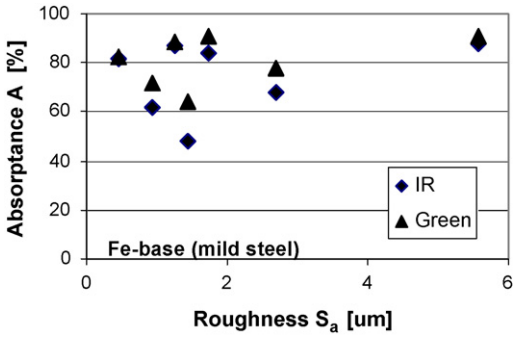

Fig. 11. Absorptance as a function of the surface roughness for the seven mild steel cases studied (Ref. values in Figs. 4–7).

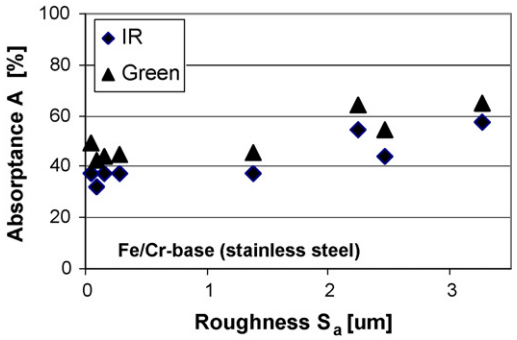

Fig. 12. Absorptance as a function of the surface roughness for the eight stainless steel cases studied (Ref. values in Figs. 8–10).

In the table below the photos the average absorptance A and standard deviation σ are given for both wavelengths as well as the results of the optical profilometry measurements[2]. Figs. 11 and 12 show the measured absorptance plotted as a function of the surface roughness for the mild and stainless steels, respectively.

3.1. Mild steels

The measured absorptance as a function of the roughness is plotted in Fig. 11 for the two wavelengths applied. No clear dependence on the roughness can be identified.

As Table 2 demonstrates, mild steel is >98% iron. However, the absorptance of cold rolled mild steel (52% at 1053 nm and 67% at 527 nm) is considerably higher than the published figure for polished iron (36% at 1053 nm and 43% at 527 nm [14]). This increase in absorptance is to be expected as our mild steel samples are not polished and are, to some extent, oxidised.

[2] Sa and Sq are the average roughness and root mean square (rms) roughness evaluated over the complete 3-D surface, respectively. If the surface is given by $Z(x,y)$, Sa and Sq are evaluated mathematically as follows:

$$\mathrm{Sa} = \iint_a |Z(x,y)|\mathrm{d}x\,\mathrm{d}y \quad \text{and} \quad \mathrm{Sq} = \sqrt{\iint_a (Z(x,y))^2 \mathrm{d}x\,\mathrm{d}y}.$$

Table 4
Reflectances of the iron oxides

Oxide	Reflectance (%)	
	λ = 1053 nm	λ = 527 nm
FeO [15]	19	20
Fe_2O_3 (hematite) [16]	31	3
Fe_3O_4 (magnetite) [17]	20	17

Table 5
A summary of the average absorptance and reflectance measurements obtained from this survey

Material	λ = 1053 nm		λ = 527 nm	
	A (%)	*R* (%)	*A* (%)	*R* (%)
MS1,2: Cold rolled mild steel (averaged)	52	48	67	33
MS3-5: Hot rolled mild steel (averaged)	86	14	89	11
MS6: Hot rolled, pickled + oiled mild steel	68	32	78	22
MS7: Hot rolled, corroded mild steel	88	12	91	9
SS1,2: Cold rolled stainless steel (averaged)	37	63	44	56
SS3,4: Hot rolled stainless steel (averaged)	56	44	65	35
SS5: Hot rolled 3Cr12	44	56	55	45
SS6,7: Bright annealed stainless steel (averaged)	35	65	46	54
SS8: Brushed stainless steel	37	63	46	54

As would be expected, the absorptance of mild steel increases with increasing levels of surface oxide. The relatively clean metal surface of cold rolled mild steel is more reflective than a pickled and oiled hot rolled surface. Hot rolled mild steel does not have a metallic surface as it is coated in a combination of iron oxides. The reflectances of FeO, Fe_2O_3 and Fe_3O_4 are shown in Table 4.

It is clear from the results that the presence of iron oxides, either as mill scale or corrosion products will increase the absorptance of the steel surface. It is also clear that the presence, or otherwise, of a thick oxide surface affects the absorptance at these two wavelengths by different amounts. For the two cold rolled samples the green light absorptance value was higher than the infrared value by 16% in one case and 34% in the other. The differences for the hot rolled, oxide coated material were considerably smaller than this, with an average value of 3%. This indicates a disproportionate rise in the absorptance at the infrared wavelength in the presence of thick layers of oxide.

3.2. Stainless steels

The measured absorptance as a function of the surface roughness is plotted in Fig. 12. In this case there are indications of a roughness–absorptance correlation at roughness values above Sa = 1.5 μm.

Comparison of the surface profilometry maps and data in Figs. 8 and 9 reveals that the hot rolled material has Sa values which are an order of magnitude greater than those for the cold

rolled material. This has resulted in higher absorptance values for the hot rolled material. The correlation between surface roughness and absorptance seems, however, to disappear at low levels of surface roughness. For example; the standard cold rolled 316SS sample has a roughness measurement which is an order of magnitude larger than the dull polished (brushed) sample but, in this case, both Sa values are below 1.5 μm and the absorptances of the two surfaces are very similar. The whole subject of roughness–absorptance correlation will be the subject of future work by the present authors.

Table 5 lists a summary of the absorptance and reflectance measurements taken in these experiments.

4. Conclusions

Reliable absorptance results have been measured for a range of mild and stainless steels for Nd:YLF and Nd:YAG lasers at their infrared and green wavelengths. These results have, as expected, been found to differ considerably from existing published data for pure, polished metals.

Several trends could be identified for the 15 ferrous samples:

- All measured absorptance values were considerably higher than the previously published ones for pure, polished metals. The increases in absorptance can be attributed to; surface oxides, surface contamination, surface roughness and the presence of alloying elements. Further studies will be needed to isolate the contributions and importance of each factor.
- The absorptance of the ferrous samples was always higher for the green wavelength compared to the infrared.
- For stainless steel a trend of increasing absorptance for increasing roughness could be seen for Sa roughness values above 1.5 μm. Below this value there was no roughness–absorptance correlation. No clear roughness–absorptance correlation was observed for the mild steel samples for Sa values below 6 μm.

References

[1] D. Bergstrom, A. Kaplan, Mathematical modelling of laser absorption mechanisms in metals: a review, in: Proceedings of the 16th Meeting on Mathematical Modelling of Materials Processing with Lasers (M^4PL16), Igls, Austria, 2003.
[2] H. Hügel, F. Dausinger, Interaction phenomena, first ed., Handbook of the Euro-Laser Academy, 2, 1998, pp. 1–102.
[3] A.M. Prokhorov, V.I. Konov, I. Ursi, I.N. Mihailescu, Laser heating of metals, Adam Hilger Series on Optics and Optoelectronics, first ed., 1990.
[4] M. von Allmen, A. Blatter, Laser-Beam Interactions with Materials, second ed., Springer, 1995.
[5] K. Blidegn, The interaction between laser light and metal, Ph.D. Thesis, Tech. University of Denmark, Copenhagen, Denmark, 1997.
[6] D.J. Price, The temperature variations of the emissivity of metals in the near infrared, Proc. Phys. Soc. 47 (1947) 131–138.
[7] D. Bergstrom, A. Kaplan, J. Powell, Laser absorptance measurements in opaque solids, in: Proceedings of the 10th Nordic Laser Materials Processing (NOLAMP) Conference, Lulea, Sweden, (2005), pp. 91–115.
[8] M. Modest, Radiative Heat Transfer, second ed., Elsevier Science, 2003.
[9] J.-F. Sacadura, Measurement techniques for thermal radiation properties, in: Proceedings of the Nineth International Heat Transfer Conference, 1990, pp. 207–222.
[10] F.J.J. Clarke, J.A. Compton, Correction methods for integrating sphere measurements of hemispherical reflectance, Color Res. Appl. 11 (1986) 253–262.
[11] Labsphere Application Note 01, Methods for single beam substitution error for integrating sphere spectroscopy accessories, www.labsphere.com.
[12] A. Seifter, K. Boboridis, A.W. Obst, Emissivity measurements on metallic surfaces with various degrees of roughness: a comparison of laser polarimetry and integrating sphere reflectometry, in: Proceedings of the 15th Symposium on Thermophysical Properties, 2003, pp. 547–560.
[13] A. Roos, C.G. Ribbing, M. Bergkvist, Anomalies in integrating sphere measurements on structured samples, Appl. Optics 27 (1988) 3828–3832.
[14] J.H. Weaver, E. Colavita, D.W. Lynch, R. Rosei, Low-energy interband absorption in bcc Fe and hcp Co, Phys. Rev. B 19 (1979) 3850–3856.
[15] T. Henning, H. Mutschke, Low-temperature infrared properties of cosmic dust analogues, Astron. Astrophys. 327 (1997) 743–754.
[16] L.A. Marusai, R. Messier, W.B. White, Optical absorption spectrum of hematite, αFe_20_3 near IR to UV, J. Phys. Chem. Solids 41 (1980) 981–984.
[17] A. Schlegel, S.F. Alvarado, P. Wachter, Optical properties of magnetite (Fe_3O_4), J. Phys. C.: Solid State Phys. 12 (1979) 1157–1164.